

# ELECTROSTATIC POTENTIAL WELLS FOR MANIPULATIONS OF DROPS IN MICROCHANNELS

R. de Ruiter, A.M. Pit, V. Martins de Oliveira, D. Wijnperlé, M.H.G. Duits, H.T.M. van den Ende, and F. Mugele

University of Twente, THE NETHERLANDS

## ABSTRACT

Precise control and manipulation of individual drops are crucial in many lab-on-a-chip applications. We present a novel hybrid concept for channel-based discrete microfluidics with integrated electrical actuation functionality. By combining the high throughput from channel-based microfluidics with individual drop control from electrical actuation we harvest the strengths of both worlds. The tunable strength of the electrostatic forces enables a wide range of drop manipulations, such as on-demand trapping and release, guiding, and sorting of drops. The conditions for trapping can be predicted using a simple model that balances the retaining electrostatic force with the hydrodynamic drag force.

**KEYWORDS:** discrete microfluidics, electrostatic force, trapping, guiding, sorting

## INTRODUCTION

In recent years several passive methods for drop trapping have been proposed, e.g. by making use of capillary valves and storage wells [1] or small holes in the microchannel wall that function as anchor [2]. Precise control over individual drops is limited, as these methods are generally non-selective and not tunable. A change in the direction or magnitude of the flow is often required to remove drops from a trap. Precise control over individual drops can be achieved via digital microfluidics (DMF), in which drops are actuated by a series of individually addressable electrodes [3]. Although high actuation speeds can be achieved in DMF, high throughputs require extensive programming of many electrodes. We combine high throughput and low sample volumes from channel-based microfluidics and individual drop control from electrical actuation by incorporating insulator-covered electrodes in the walls of microchannels. The depth of the electrostatic potential well is tunable *via* the voltage, allowing for the implementation of several drop operations.

## THEORY

The potential well as generated by two co-planar electrodes separated by a gap has been described by 't Mannetje *et al.* [4] for spherical-cap shaped drops resting on a surface. The same analysis can be used for drops that are confined between the bottom and top walls of a microchannel, where the drop radius  $R$  in the horizontal plane is much larger than the channel height  $h$  (Figure 1). Briefly, when a drop of electrically conductive liquid capacitively couples to both electrodes, an electrical circuit containing two parallel plate capacitors in series is formed. The overall capacitance is  $C(x) = C_1(x)C_2(x)/(C_1(x) + C_2(x))$ , where the individual capacitances are given by  $C_{1,2}(x) = (\epsilon_0\epsilon_d/d)A_{1,2}(x)$ . Here,  $c = \epsilon_0\epsilon_d/d$  is the capacitance per area of the dielectric layer and  $A_{1,2}(x)$  is the area of the drop above the respective electrode (Figure 1b). Charging the capacitors by applying a voltage  $U$  generates an electrostatic free-energy landscape  $E_{el}(x) = -C(x)U^2/2 = -cAU^2f(x)$  (Figure 1c), with  $A = \pi R^2$  the total contact area of the drop. The dimensionless function  $f(x)$  can be derived from geometry and accounts for the variations in the areas. The corresponding trapping force  $F_{el}(x) = -dE_{el}(x)/dx$  has a maximum value  $F_{el,max} = -acRU^2$ . We thus find that the maximum trapping force scales with the capacitance per area, the drop radius, and the voltage squared, with a proportionality constant  $a$  that depends on the electrode configuration.

Various electrode configurations are possible. A gap that runs parallel to the flow direction in between two finite electrodes has the benefits of keeping drops on a predefined track and confining the trapped drop to a specific position. The hydrodynamic forces will push the drop towards the edge of the electrodes, and the area of the drop above the electrodes decreases as the drop is passing the trap. The maximum electrostatic trapping force is now given by

$$F_{el,max} = -(1/4)cRU^2, \quad (1)$$

assuming that the gap width  $g$  is negligible.  $F_{el,max}$  is reached when the drop is halfway the edge of the electrodes.

The hydrodynamic drag force exerted by the outer flow is obtained from the Stokes equation. The microchannel can be modeled as a Hele-Shaw cell, where the problem is reduced to a 2D flow by averaging the velocity field over the microchannel height. Analytical calculation of the drag force on a cylinder with no-slip boundary condition in an infinitely wide channel yields

$$F_{drag} = (24\pi\mu R^2/h)(1 + 2K_1(q)/(qK_0(q))), \quad (2)$$

with  $\mu$  the viscosity of the continuous phase,  $K_0$  and  $K_1$  modified Bessel functions of the second kind and  $q = 2\sqrt{3}R/h$ .

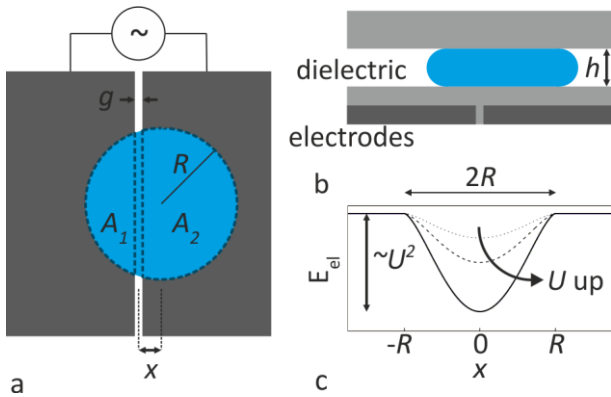


Figure 1: (a) Top view and (b) side view of a co-planar electrode design. (c) Electrostatic potential well.

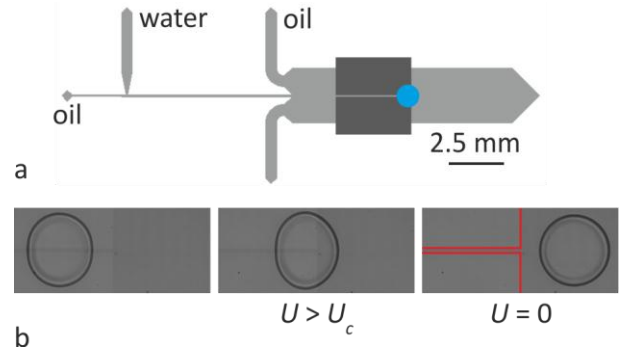


Figure 2: (a) Overview of the device. (b) On demand trapping ( $U > U_c$ ) and release ( $U = 0$ ) of a drop.

## EXPERIMENTAL

The microchannels are fabricated from polydimethylsiloxane (PDMS, Sylgard 184). Figure 2a gives an overview of the device, which consists of a tapered T-junction where aqueous drops are formed and a main channel (height  $85 \mu\text{m}$ , width  $2.5 \text{ mm}$ ) containing the electrodes. The side inlets are used to control the oil flow rate in the main channel. Patterned electrodes in the bottom substrate are obtained by photolithography and etching of indium tin oxide (ITO), creating gaps of  $15 \mu\text{m}$ . PDMS is spin coated to obtain a  $\sim 7 \mu\text{m}$  thick insulating layer that separates the drops from the electrodes. The PDMS is partly cured and subsequently sealed to the microchannels. The properties of the dielectric layer are determined from the electrowetting response [5]; the capacitance per area is determined to be  $c = 2.5 \cdot 10^{-6} \text{ F/m}^2$ .

Paraffin oil ( $\mu = 100 \text{ mPa}\cdot\text{s}$ ) is used as the continuous phase, and the dispersed phase consists of de-ionized water (Millipore Synergy UV,  $18.2 \text{ M}\Omega\text{cm}$ ) with KCl added up to a conductivity of  $3 \text{ mS/cm}$ . The interfacial tension of the water/oil interface is  $50 \text{ mN/m}$ . Continuous oil flows are driven using syringe pumps. The dispersed phase is brought to the T-junction by adjusting the water pressure. Drops are formed on demand by generating short air-pressure pulses using a pressure regulator. An alternating voltage ( $f = 1 \text{ kHz}$ ,  $U = 0\text{-}350 \text{ V}$ ) is applied between the two separated electrodes in the main channel to generate electrostatic forces on the drops.

## RESULTS AND DISCUSSION

To examine the trapping capability of our split-electrode configuration, we formed drops of  $R = 150 \mu\text{m}$  at various voltages and determined drop trajectories (Figure 3). All drops have the same initial velocity. When no voltage is applied, the drop traverses the microchannel without changing its velocity. At low voltages the drop decelerates when it starts crossing the edge of the electrodes, and accelerates back to the initial velocity after leaving the trap. Trapping of the drop only occurs when the voltage exceeds a critical value  $U_c$ . The drop is slowed down until a zero velocity is attained at a voltage-dependent trapping position, and can afterwards be released on demand by switching off the voltage (Figure 2b).

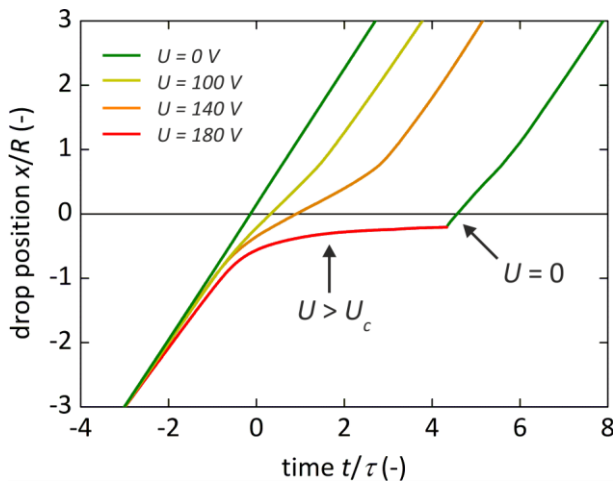


Figure 3: Drop trajectories upon passing the trap for various applied voltages.

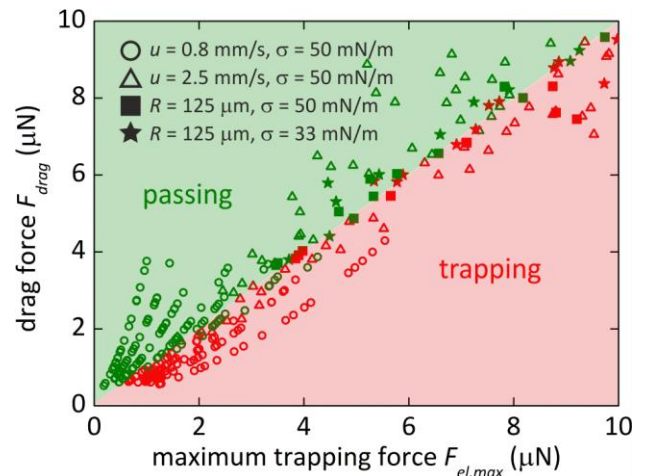


Figure 4: Drag force versus maximum trapping force. The open and closed symbols represent experiments at fixed flow velocity and fixed drop size, respectively.

We performed systematic experiments to investigate how this critical voltage  $U_c$  depends on the size of the drops. The drop size ( $R = 50\text{-}250 \mu\text{m}$ ) and the applied voltage ( $100\text{-}350 \text{ V}$ ) were varied independently, while the flow rate of

the continuous phase in the test section with the trap was held constant. The results show that  $U_c$  increases with  $R$ , which means that the trap is size-selective; for each given voltage we find a critical drop radius  $R_c$  above which the drop cannot be trapped anymore. Extending the measurements to different oil flow rates and different oil/water interfacial tensions (by using a mixture of ethylene glycol and water), we found that the critical voltage increases with flow rate while it does not depend on the interfacial tension.

To explain the dependence of the critical voltage on drop size and flow rate (but not on interfacial tension) we consider the balance between the maximum electrostatic trapping force and the hydrodynamic driving force on the drop. Using equation (1) for the maximum trapping force and equation (2) for the drag force we find that the transition from passing to trapping is observed when both forces are similar in magnitude for a wide range of experimental conditions. Although deviations from a quantitative correspondence can be expected due to drop deformations on the trap (Figure 2b), additional contributions to the electrostatic and interfacial energy due to a voltage-dependent contact angle decrease [5], and breakdown of the Hele-Shaw approximation in the determination of the drag force, the agreement with the model is certainly good enough for the design of trapping experiments.

The principle that the electrostatic force will pull a drop towards the middle of a gap, can also be used to direct drops. By combining several electrodes in a branching geometry, drops can be guided laterally along various predefined tracks, depending on which electrodes are activated (Figure 5). The path of subsequent drops can be easily altered by switching between the electrodes. To achieve high-speed sorting we designed a three-electrode branching geometry underneath a Y-shaped channel (height  $55\mu\text{m}$ , width  $200\mu\text{m}$ ). We generated water drops in silicon oil ( $\mu = 30\text{ mPas}$ ) using a flow focusing device. An AC potential difference ( $f = 10\text{ kHz}$ ,  $U = 225\text{ V}$ ) is applied continuously across the upper and lower electrodes, while the middle electrode is switched between applied potential and ground, effectively switching the path of the drop from one outlet to the other (Figure 6). Modulating the middle electrode at half the frequency of drop generation allows alternately sorting of drops. With the current device and materials used, we are able to sort at 100 drops per second. In combination with a detection technique, e.g. optical or electrical, our device could be used as an active sorter.

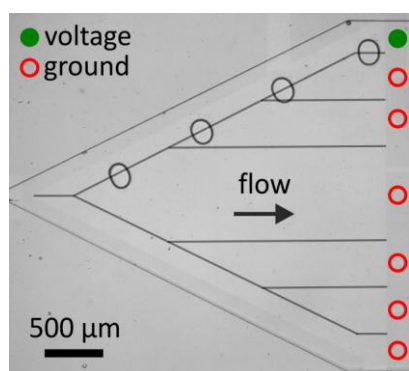


Figure 5: Guiding of drops (superposition at various times).

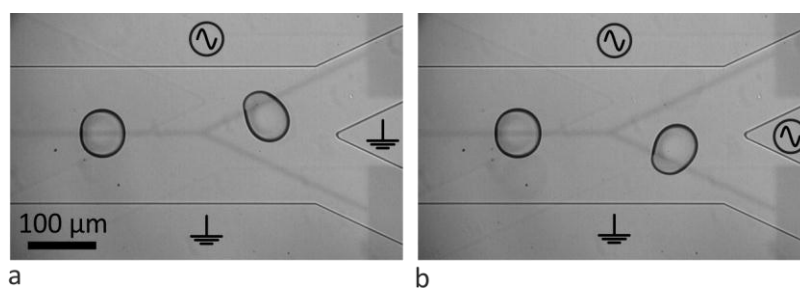


Figure 6: Sorting of drops. Drops are directed (a) to the upper channel when the middle electrode is grounded and (b) to the lower channel when a voltage is applied.

## CONCLUSION

We presented a hybrid concept for channel-based microfluidics with integrated electrical actuation functionality to achieve individual control over nanoliter aqueous drops at high throughput. The trapping of drops by a co-planar electrode configuration is successfully predicted using a simple model that balances the maximum electrostatic force exerted by the trap with the hydrodynamic drag force exerted by the surrounding flow. In addition, we showed guiding and high-speed sorting of drops.

## ACKNOWLEDGEMENTS

This research is supported by BP and by the Dutch Technology Foundation STW, which is part of the Netherlands Organisation for Scientific Research (NWO), and which is partly funded by the Ministry of Economic Affairs.

## REFERENCES

- [1] H. Boukellal, S. Selimovic, Y. W. Jia, G. Christobal, and S. Fraden, *Lab. Chip.*, 2009, 9, 331-338.
- [2] R. Dangla, S. Lee, and C. N. Baroud, *Phys Rev. Lett.*, 2011, 107, 124501.
- [3] M. G. Pollack, R. B. Fair, and A. D. Shenderov, *Appl. Phys. Lett.*, 2000, 77, 1725-1726.
- [4] D. J. C. M. 't Mannetje, A. G. Banpurkar, H. Koppelman, M. H. G. Duits, H. T. M. van den Ende, and F. Mugele, *Langmuir* in press, DOI:10.1021/la4015724.
- [5] F. Mugele and J. C. Baret, *J. Phys. Condens. Matter*, 2005, 17, R705-R774.

## CONTACT

\*R. de Ruiter, r.deruiter-1@utwente.nl